



ELSEVIER

Available online at www.sciencedirect.com

SCIENCE @ DIRECT®

Journal of Organometallic Chemistry 687 (2003) 85–99

Journal
of Organometallic
Chemistry

www.elsevier.com/locate/jorganchem

Synthesis and characterisation of Pd(II) complexes with a derivative of aminoazobenzene

Dynamic ¹H-NMR study of cyclopalladation reactions in DMF

Manda Čurić^{a,*}, Darko Babić^a, Željko Marinić^a, Ljiljana Paša-Tolić^b,
Vjera Butković^a, Janez Plavec^c, Ljerka Tušek-Božić^a

^a Ruder Bošković Institute, Bijenicka 54, HR-10002 Zagreb, Croatia

^b Pacific Northwest National Laboratory, 902 Battelle Boulevard, Richland, WA 99352, USA

^c NMR Center, National Institute of Chemistry, Hajdrihova 19, SI-1001 Ljubljana, Slovenia

Received 26 March 2003; received in revised form 21 July 2003; accepted 21 July 2003

Abstract

Three new Pd(II) complexes, i.e. [PdCl₂L]₂ (**A**), PdCl₂L₂ (**B**) and [Pd(μ-Cl)(L-H)]₂ (**C**), each with two diethyl [α-(4-benzenazoanilino)-2-hydroxybenzyl]phosphonates (**L**) bound to either one or two palladium atoms, are synthesized and characterized by elemental analysis, by IR, UV–vis and solid-state ¹³C-NMR spectra. Complexes **B** and **C** are additionally characterized by ¹H-, ¹³C- and ³¹P-NMR and electrospray mass spectrometry (ESMS) studies using dimethylformamide (DMF) as a solvent. In DMF solution adducts **A** and **B** undergo spontaneous rearrangement into the cyclopalladated complex **C**. Dynamic ¹H-NMR study of this rearrangement as well as of the reactions of **L** with PdCl₂ and Na₂PdCl₄ revealed a complex equilibrium in DMF solutions and enabled the formation mechanism of all involved species to be resolved. The complex **A** is immediately solvolyzed producing two molecules of intermediate **M** [PdCl₂(L)(DMF)]. Complex **M** was also the first intermediate in the reaction of **L** with PdCl₂. Once present in concentration above 10⁻⁵ mol dm⁻³ **M** dimerizes very fast into chloro-bridged dimer [PdCl(μ-Cl)(L)]₂ (**D**) which undergoes cyclopalladation and converts into the complex **C**. The formation of **C** from the intermediate **D** is clearly demonstrated by the concentration dependence of the cyclopalladation reaction which has order greater than one. Chloride ions, released by cyclopalladation, react with **D** by splitting chloro-bridge and binding to metal atoms to produce byproduct [PdCl₃(L)]⁻ (**T**). The same species **T** are formed in the reaction of **L** with Na₂PdCl₄ whereby a chloride ion is replaced by the ligand **L**. The complex **B** undergoes similar, but slower, solvolytic reaction producing **M** and **L** while further reaction steps are identical as in the solvolysis of **A**.

© 2003 Elsevier B.V. All rights reserved.

Keywords: Palladium; Azobenzenes; Cyclopalladation; ¹H-NMR study; Dynamics

1. Introduction

Preparation of cyclopalladated complexes has attracted considerable attention by a number of research groups due to their potential application in organic synthesis [1], homogenous catalysis [2], photochemistry [3], optical resolution [4], and also in the design of new metallomesogenes [5] and antitumor drugs [6]. Particularly interesting are complexes with N-donor ligands,

due to their easy orthometallation by Pd(II) salts [7]. One of the first examples of cyclopalladation reaction was reported for azobenzene [8]. Later it was found that Pd(II) complexes may undergo cyclopalladation reactions with other N-donor ligands [7] too.

Reaction mechanisms and kinetics of cyclopalladation reactions have been recently resolved with *N*-benzylamines [9], *N*-benzyltriamines [10], *N*-benzylideneamines [11] and 2-phenylpyridines [12] as N-donor ligands. Still, a very little is known about the mechanism and reaction dynamics of cyclopalladation reaction with azobenzenes [13], although the first complexes have been prepared more than 30 years ago. Bruce et al. [14] have

* Corresponding author. Fax: +385-1-4680084.

E-mail address: curic@rudjer.irb.hr (M. Čurić).

demonstrated that the palladium atom acts as an electrophile since the favoured site of attack in asymmetrically substituted azobenzenes is the aromatic ring with an electron-releasing group. It is commonly assumed that the first step in the cyclopalladation reaction is coordinative bonding of the azo-nitrogen to the palladium atom [13a,14,15]. Though this assumption is quite logical, a direct experimental proof is still lacking.

In this paper we report on the synthesis and characterization of new mononuclear and binuclear Pd(II) complexes, i.e. PdCl₂L₂ (**B**), [PdCl₂L]₂ (**A**) and [Pd(μ-Cl)(L-H)]₂ (**C**) where ligand **L** is diethyl [α-(4-benzenazoanilino)-2-hydroxybenzyl]phosphonate (Fig. 1) and L-H is produced by release of proton from **L** (Scheme 1). Synthesis and characterization of new Pd(II) complexes is a part of our long-term efforts to prepare a new class of potential antitumor and antiviral agents [16]. An unexpected spontaneous conversion of the binuclear **A** as well as mononuclear **B** complex into the chloro-bridged binuclear cyclopalladated complex **C** was observed during their characterization in dimethylformamide (DMF). A detailed investigation has been performed to resolve the mechanism of these transformations and results are reported in this paper. The new insight into the transformation of adducts into the binuclear cyclopalladated complex and particularly into the mechanism of cyclopalladation reaction of 4-aminoazobenzene derivative will enable the rational design and synthesis of a new generation of Pd(II) complexes with N-donor ligands.

2. Experimental

2.1. General methods

Infrared spectra were recorded on a Perkin–Elmer 580 B and on a FT Perkin–Elmer 2000 spectrophotometers using KBr pellets (4000–250 cm⁻¹) and Nujol mulls in polyethylene (400–200 cm⁻¹). Visible and ultraviolet spectra were taken on a Cary 219 spectrophotometer with thermostated cell compartment and a Hewlett–Packard 8452A spectrophotometer. ¹H-, ¹³C- and ³¹P-NMR data were recorded in DMF-*d*₇ solvent by using Varian Gemini 300 FT NMR spectrometer operating at 300.08, 75.54 and 121.44 MHz for ¹H, ¹³C and ³¹P nuclei, respectively. ³¹P-NMR spectra were

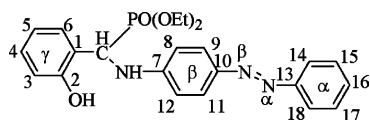
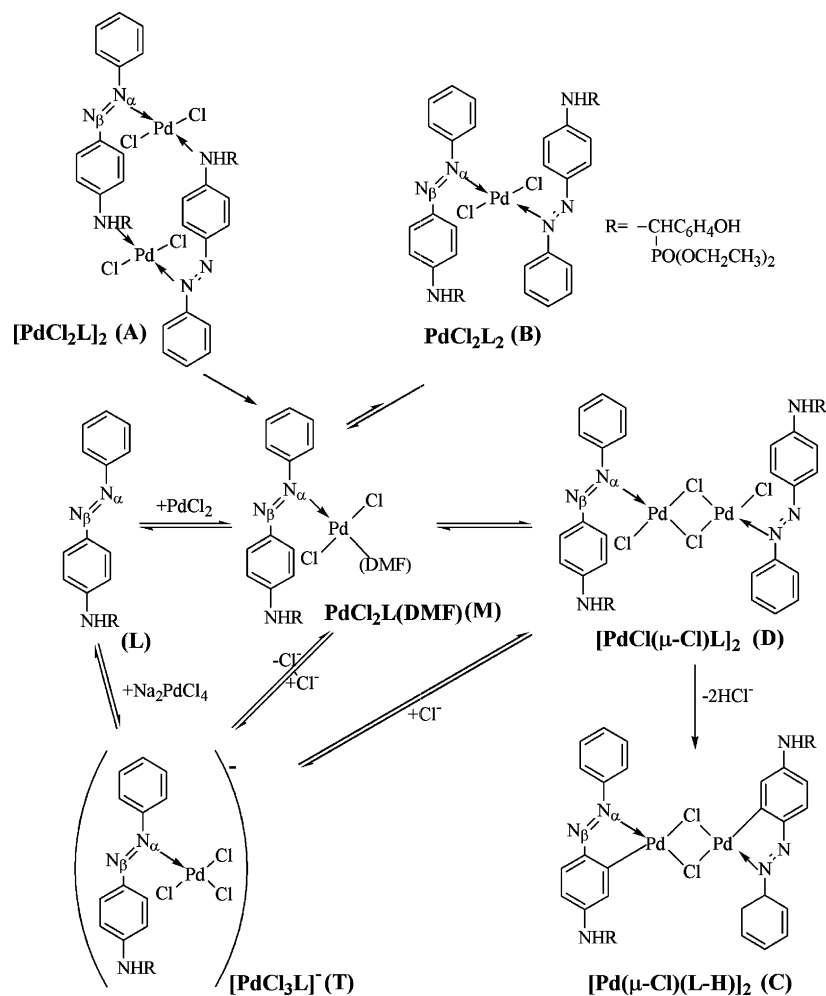


Fig. 1. Diethyl[α-(4-benzenazoanilino)-2-hydroxybenzyl]phosphonate (**L**).

recorded by using 85% H₃PO₄ as external standard ($\delta = 0.00$ ppm). The ¹H-¹H COSY and ¹H-¹³C-HSQC spectra were recorded by using Bruker Avance DRX 500 NMR spectrometer. The ¹H-¹H COSY spectra were recorded using 1 K in F2 dimension and 256 increments in F1 dimension. The latter were zero filled to 1 K. Each increment was obtained with eight transients using 6000 Hz spectral width. The ¹H-¹³C HSQC spectra were measured with one-bond C–H coupling value set to 140 Hz, using 2 K in F2 dimensions and 256 increments in F1 dimension. The latter were zero-filled to 1 K. Increments were obtained using 256 transients. Spectral widths were 31,250 Hz in F2 and 6000 Hz in F1 dimension. Solid-state ¹³C-NMR experiments were carried out at 76.19 MHz on Varian Unity plus spectrometer operating at a field of 7T using cross-polarization (CP) and magic angle spinning (MAS) with high power ¹H decoupling. The ¹³C CP-MAS spectra were obtained with a 4 ms CP contact time and 1 s recycle time. The spinning rate using 7 mm Doty Scientific probe was ca. 4 kHz. The 7 tesla ESI Fourier Transform ion cyclotron resonance mass spectrometer used for the present study has been described in detail elsewhere [17]. An atmospheric ESI source comprises a stainless steel heated capillary inlet to the mass spectrometer that incorporates an electrodynamic ion funnel assembly to improve ion transmission through interface followed by a collisional focusing quadrupole. The compounds were dissolved in DMF and this solution was injected directly into the mass spectrometer at a flow rate of 0.3 $\mu\text{l min}^{-1}$ in a pulled glass capillary. A source potential of ca. 2 kV was applied to produce a stable ion current, while the heated capillary was maintained at 200 V and 60–120 °C. Ions were transferred from the ESI interface to the ICR trap using an rf-quadrupole ion guide for collisional focusing at 200 mtorr, followed by two sets of rf-only quadrupole ion guides in the higher vacuum regions of the mass spectrometer. Ion accumulation was accomplished by introducing N₂ into the FTICR trap at the pressure of 10⁻⁵ torr *via* a piezoelectric valve (Lasertechniques Inc., Albuquerque, NM). Background pressure in the ICR trap was maintained at 10⁻⁹ torr using a custom cryopumping assembly. Mass spectra were acquired using a standard experimental sequence for ion injection and accumulation, pump-down, excitation, and detection. The analysis of the FTICR spectra was performed using ICR-2LS software [18]. X-ray diffraction powder data were obtained using Cu–K α radiation ($l = 1.5406$ Å) on a Philips PW 3710 diffractometer. Data were collected in the $3 < 2\theta < 65^\circ$ range, in the $\theta - 2\theta$ step scan mode with $\Delta 2\theta = 0.02^\circ$ and $t = 12$ s. Magnetic susceptibilities were determined by the standard Gouy method at 23 °C using CuSO₄·5H₂O for calibration.



Scheme 1.

2.2. Materials

Diethyl $[\alpha\text{-}(4\text{-benzenazoanilino})\text{-}2\text{-hydroxybenzyl}]\text{phosphonate}$ [19] and dichlorobis(acetonitrile) palladium(II) [20] were prepared according to a literature procedures. All other chemicals and solvents were of reagent grade and used without further purification. IR of **L** (KBr pellet, cm^{-1}): 3294 (ms, $\nu_{\text{N-H}}$), 1601 (s, δ_{NH} and $\nu_{(\text{C}=\text{C})_{\text{ar}}}$), 1233 (s, $\nu_{\text{P}=\text{O}}$). ^{31}P -NMR, 25.65 ppm (1P). ^{13}C CP-MAS NMR, 18.2 ppm (CH_3 , 2C), 48.6 ppm (PCH, 1C), 63.6 ppm (OCH_2 , 2C), 109.5–134.5 ppm ($\text{C}_{\text{ar}}\text{-H}$ and **C-1**, 14C), 140.5–158.0 ppm (**C-2,7,10,13**, 4C).

2.2.1. Preparation of $[\text{PdCl}_2\text{L}]_2$ (**A**)

Trans- $\text{PdCl}_2(\text{CH}_3\text{CN})_2$ (90 mg, 0.34 mmol) was dissolved in warm dichloromethane (10 ml) and added to the solution of 150 mg (0.34 mmol) of **L** in dichloromethane (5 ml). The reaction mixture was refluxed for 3 h. The yellow precipitate was filtered off, washed with dichloromethane and dried under vacuum at room temperature (r.t.). Yield 31%. Anal. Calc. (Found) for

$\text{C}_{46}\text{H}_{52}\text{Cl}_4\text{N}_6\text{O}_8\text{P}_2\text{Pd}_2$: C, 44.78 (44.39); H, 4.26 (4.58); N, 6.81 (7.10); Pd, 17.25 (17.41). IR (KBr pellet, cm^{-1}): 3070 (w-m, $\nu_{\text{N-H}}$), 1601 (m, δ_{NH} and $\nu_{(\text{C}=\text{C})_{\text{ar}}}$), 1229 (s, $\nu_{\text{P}=\text{O}}$); (Nujol mull in polyethylene): 341 (w, $\nu_{\text{Pd-Cl}}$). ^{31}P -NMR of **D**, 25.46 ppm (2P). ^{13}C CP-MAS NMR, 16.2, 18.7 ppm (CH_3 , 4C), 63.6, 64.8 ppm (OCH_2 , 4C), these two signals overlapped with PCH signal, 115.0–138.0 ppm ($\text{C}_{\text{ar}}\text{-H}$ and **C-1**, 28C), 142.5–159.0 ppm (**C-2,7,10,13**, 8C).

2.2.2. Preparation of PdCl_2L_2 (**B**)

Trans- $\text{PdCl}_2(\text{CH}_3\text{CN})_2$ (92 mg, 0.35 mmol) was dissolved in warm dichloromethane (10 ml) and added to the solution of **L** (300 mg, 0.70 mmol) in dichloromethane (5 ml). The reaction mixture was refluxed for 5 h. The red precipitate was filtered off, washed with dichloromethane and dried under vacuum. Yield 50%. Anal. Calc. (Found) for $\text{C}_{46}\text{H}_{52}\text{Cl}_2\text{N}_6\text{O}_8\text{P}_2\text{Pd}$: C, 52.30 (52.35); H, 4.97 (4.72); N, 7.96 (7.90); Pd 10.07 (9.92). IR (KBr, cm^{-1}): 3320 (m, $\nu_{\text{N-H}}$), 1601 (s, δ_{NH} and $\nu_{(\text{C}=\text{C})_{\text{ar}}}$), 1235 (s, $\nu_{\text{P}=\text{O}}$); (Nujol mull in polyethylene): 340 (w, $\nu_{\text{Pd-Cl}}$). ^{31}P -NMR, 25.63 ppm (2P). ^{13}C CP-

MAS NMR, 14.7 ppm (CH₃, 4C), 47.3 ppm (PCH, 2C), 62.4 ppm (OCH₂, 4C), 107.5–137.5 ppm (C_{ar}-H and C-1, 28C), 142.5–159.5 ppm (C-2,7,10,13, 8C).

2.2.3. Preparation of [Pd(μ-Cl)(L-H)]₂ (C)

A methanolic solution (10 ml) of **L** (300 mg, 0.70 mmol) was added dropwise to a methanolic solution (15 ml) of Na₂PdCl₄ (200 mg, 0.68 mmol). The resulting mixture was stirred continuously at r.t. for 5 days. The brown-red precipitate was filtered off, washed first with water and then with cold methanol and dried under vacuum. Yield 55%. Anal. Calc. (Found) for C₄₆H₅₀Cl₂N₆O₈P₂Pd₂: C, 47.60 (47.30); H, 4.35 (4.48); N, 7.96 (7.90); Pd, 18.33 (17.98). IR (KBr, cm⁻¹): 3360 (m, ν_{N-H}); 1579 (vs, δ_{NH} and ν_{(C-C)ar}), 1229 (s, ν_{P=O}); (Nujol mull in polyethylene): 314 and 295 (vw, ν_{Pd-Cl}). ³¹P-NMR, 25.66 ppm (2P). ¹³C CP-MAS NMR, 16.1 ppm (CH₃, 4C), 46.2 ppm (PCH, 2C), 64.2 ppm (OCH₂, 4C), 105.0–132.0 ppm (C_{ar}-H and C-1, 28C), 144.5–160.0 ppm (C-2,7,10,13, 8C).

2.3. Dynamic measurements

The rearrangement dynamics of dissolved complexes **A** and **B**, and of reactions of **L** with Pd(II) compounds, were monitored by ¹H-NMR spectroscopy on the Varian Gemini 300 FT NMR spectrometer. ¹H spectra were collected by using a spectral width of 4700 Hz, a number of transients 12, a pulse width of 5 μs (30°), an acquisition time of 2.54 s and no time delay. To follow the rearrangement dynamics of complexes **A** and **B**, the complexes (4.9 mg, 4.0 × 10⁻³ mmol of **A** and 14.8 mg, 1.4 × 10⁻² mmol of **B**) were dissolved in 1.0 ml DMF-*d*₇. Spectra were accumulated at various time intervals (1, 2, 4, 8 and 16 min). To monitor the reaction of the ligand **L** with Pd(II) compounds, the following three reaction mixtures were prepared in DMF-*d*₇ (1.0 ml): (a) **L** (11.2 mg, 2.6 × 10⁻² mmol) with PdCl₂ (4.7 mg, 2.7 × 10⁻² mmol); (b) **L** (8.5 mg, 1.9 × 10⁻² mmol) and *trans*-PdCl₂(Me₂SO)₂, (6.0 mg, 1.8 × 10⁻² mmol); and (c) **L** (4.3 mg, 9.8 × 10⁻³ mmol) with Na₂PdCl₄ (9.38 mg, 2.7 × 10⁻² mmol). Spectra were collected at either 1, 2, 4, 8 and 16 min intervals. All reactions were monitored at 18 ± 1 °C in 5 mm NMR tube.

The former reactions were also monitored by UV-vis spectroscopy on a HP 8452A spectrophotometer in the range 260–750 nm at 25 °C. The rearrangement dynamics of **A** and **B** were followed by using two concentrations of each complex (9.7 × 10⁻⁶ and 9.8 × 10⁻⁵ mol dm⁻³ of **A**; 1.2 × 10⁻⁵ and 1.18 × 10⁻⁴ mol dm⁻³ of **B**). To follow the interaction of **L** with Pd(II) compounds, two reaction mixtures were prepared (1 × 10⁻⁵ and 1 × 10⁻⁴ mol dm⁻³ of **L** and PdCl₂). Spectra of all reactions were accumulated for 15 h at various time intervals (0.25, 0.5, 1, and 10 min). The cell

thicknesses were 0.1 and 1 cm depending on the Pd(II) compounds and **L** concentrations.

3. Results and discussion

3.1. Synthesis and characterization

[PdCl₂L]₂ (**A**) and PdCl₂L₂ (**B**) complexes were obtained in CH₂Cl₂ by reaction of **L** with PdCl₂(CH₃CN)₂ in 1:1 and 1:2 metal:ligand ratio, respectively. The yield of **A** (31%) is low due to concurrent reactions that end up with the complex **C** which is more soluble in CH₂Cl₂ than **A** and **B**. The dimeric complex [Pd(μ-Cl)(L-H)]₂ (**C**) was prepared in methanol by the reaction of equimolar amounts of **L** and Na₂PdCl₄.

The structural assignments of complexes are based on their elemental analysis, spectroscopic studies (IR, UV-vis, electrospray mass spectrometry (ESMS), solid-state ¹³C-NMR as well as ¹H-, ¹³C- and ³¹P-NMR in DMF). In comparison with **B** and **C**, **A** is either insoluble or when soluble, undergoes rapid decomposition which prevents common structural characterization (¹H-, ¹³C- and ³¹P-NMR and ESMS). From the whole body of collected data, presented and discussed here, we proposed structures of complexes **A**, **B** and **C** (Scheme 1).

All complexes are stable in air and only slightly soluble in common organic solvents (CHCl₃, CH₃OH, CH₃CN, etc.). The complexes **A** and **B** rearrange into **C** in the solvents of poor co-ordinating ability, i.e. CHCl₃ or CH₃OH while in dimethyl sulfoxide (DMSO) and CH₃CN, a strong S- and N-donor towards palladium, ligands are replaced by solvent molecules. Low solubility of **A** and **B** in CHCl₃ and CH₃OH prevent more detailed study of the rearrangement reactions in these solvents. In DMF, the results of dissolving **A** and **B** strongly depend on their concentrations. At concentrations close to 10⁻⁵ mol dm⁻³ the reaction of ligand replacement by solvent molecules is dominant while at concentrations close to 10⁻⁴ mol dm⁻³ rearrangement into **C** and decomposition to **L** are concurrent processes. At even higher concentrations of **A** or **B** the formation of **C** is preferred and consequently we tried to synthesize **C** directly from **A** and **B** in DMF. Unfortunately, it was impossible to isolate pure **C** due to simultaneous formation of byproduct in both reactions as well as ligand in the reaction from **B**.

The intermediates [PdCl(μ-Cl)L]₂ (**D**), [PdCl₂(L)(DMF)] (**M**), [PdCl₂(L)(DMSO)] (**M**^{*}) and byproduct [PdCl₃(L)]⁻ (**T**) were observed in the rearrangement reactions of **A** and **B** into **C** and in the reactions of **L** with Pd(II) compounds in DMF. Their structures, resolved by the combination of ¹H- and ¹³C-NMR, UV-vis and ESMS studies, are given in the rearrangement (Scheme 1). All attempts to isolate

intermediate **D** were unsuccessful since we always obtained the mixture of **D** and **C** species, as confirmed by $^1\text{H-NMR}$ spectroscopy.

3.1.1. IR spectra

The infrared spectra of **A**, **B** and **C** strongly indicate different modes of ligand bonding to palladium. The most significant differences were observed for the following vibration modes: (i) N–H stretching vibration ($3000\text{--}3300\text{ cm}^{-1}$); (ii) NH bending vibration and benzene ring stretching vibrations ($1500\text{--}1610\text{ cm}^{-1}$); and (iii) Pd–Cl stretching vibrations ($200\text{--}400\text{ cm}^{-1}$).

The presence of Pd–N(amino) bond in **A** is confirmed by the considerably reduced frequency and intensity of the N–H stretching vibration (from 3294 in free ligand to 3070 cm^{-1} in **A**). In addition, the reduced intensity of NH bending vibration relative to the free ligand is also detected. The same was observed in Pd(II) complexes with anilinobenzylphosphonates as ligands in which metal atom is coordinated by amino-nitrogen [**16c**]. In complexes **B** and **C** these NH frequencies are similar to those in the free ligand excluding the coordination through the amino nitrogen in these complexes.

A single $\nu(\text{Pd-Cl})$ vibration in the far infrared region (at about 340 cm^{-1}) of **A** and **B** indicates *trans* position of chlorine atoms. The presence of only one $\nu(\text{Pd-Cl})$ vibration band in the spectrum of **A** indicates that **A** and **D** are structurally different species, with the same elemental composition. The spectrum of intermediate **D** (not isolated as pure compound) must have three $\nu(\text{Pd-Cl})$ vibration bands [**21**]. Additional arguments for different structures of **A** and **D** are obtained from the solid-state $^{13}\text{C-NMR}$ spectra of complexes and from the reaction dynamics of complex **A**. The chloro-bridged complex **C** exhibits two absorptions at 314 and 295 cm^{-1} assigned to the bridging $\nu(\text{Pd-Cl})$ vibrations. The other vibrational frequencies of **B** and **C** are in agreement with those observed for structurally similar complexes of azobenzenes [**16c,16e,22**] (see Section 2).

For all complexes the position of P=O stretching vibration is almost identical as in free ligand excluding the possibility of coordination through the phosphoryl oxygen (see Section 2).

3.1.2. UV-vis spectra

The electronic absorption spectra of **L**, **A**, **B** and **C** recorded in DMF and/or CHCl_3 are summarized in Table 1. The spectra of **A** and **B** were always recorded with freshly prepared solutions since they undergo decomposition and/or rearrangement. The spectrum of **T** in DMF, obtained by recording 15 h old reaction solution of **L** and Na_2PdCl_4 , is also given in Table 1.

The spectrum of **L** in DMF exhibits a strong and rather broad absorption band at 400 nm which is assigned to the spin-allowed $\pi\text{--}\pi^*$ transition. This strong and broad band overlaps a weak, spin-allowed

Table 1
UV-vis spectral data

Compound ^a	λ_{max} , nm (ϵ , $\text{M}^{-1}\text{ cm}^{-1}$)	Solvent
L	400 (2.9×10^4), 272 (1.1×10^4)	DMF
	383 (2.7×10^4), 263 (1.0×10^4)	CHCl_3
A	455 (1.5×10^4) ^b , 413 (1.5×10^4) ^b , 318 (2.9×10^4), 280 (2.2×10^4) ^c	CHCl_3
	B ^d	480 (6.9×10^4), 310 (1.5×10^4) ^c , 272 (2.9×10^4)
444, 268		CHCl_3
C	520 (5.7×10^4), 385 (2.0×10^4), 310 (2.4×10^4), 286 (2.5×10^4)	DMF
	500 (4.0×10^4), 393 (1.9×10^4), 332 (1.8×10^4), 298 (2.3×10^4), 277 (2.2×10^4)	CHCl_3
M ^e	464 (3.5×10^4), 277 (1.8×10^4)	DMF
T	451 (3.4×10^4), 279 (1.9×10^4)	DMF

^a The spectra of **A** and **B** were recorded with the freshly prepared solutions.

^b This band probably corresponds to the ligand transitions of other species present in the solution.

^c Shoulder.

^d Since **B** is very weakly soluble in CH_3Cl it was impossible to determine the extinction coefficients.

^e The spectrum obtained by dissolving **A** at initial concentration $10^{-5}\text{ mol dm}^{-3}$ corresponds to the first intermediate **M**.

$n\text{--}\pi^*$ transition which is expected in the same region [**23**]. A prominent band observed at 272 nm is assigned to the second $\pi\text{--}\pi^*$ transition [**23**] (Fig. 2a). The same absorption bands also occur in CHCl_3 (383 and 263 nm).

An additional support for the presence of Pd–N(amino) bond in **A** is given by its spectrum in CHCl_3 , which possesses a strong band at 318 nm , assigned to the $\pi\text{--}\pi^*$ transition of the bound ligands (Fig. 2b). This transition is considerably shifted to higher energy with respect to the corresponding transition in the free ligand **L** (383 nm) and **B** (444 nm). The position and intensity of the $\pi\text{--}\pi^*$ transition suggest that there is no conjugation of the phenylazo group with amino group when palladium atom is bound to it. Since, in CHCl_3 **A** also rearranges into **C**, the two overlapping bands at 413 and 455 nm , with complex temporal dynamics, probably correspond to the ligand transitions of other species present in the solution (Fig. 2b).

The spectrum of **A** in DMF could not be obtained due to its immediate solvolysis into **M**. The initial spectrum obtained by dissolving **A** in DMF is characterized by a very strong absorption at 464 nm which is assigned to transitions of the bound ligand: spin-allowed $\pi\text{--}\pi^*$ and $n\text{--}\pi^*$. The position of this $\pi\text{--}\pi^*$ transition (red shifted in comparison with the corresponding maximum of **L**) suggests immediate breaking of two Pd–N(amino) bonds in **A** in DMF and its decomposition into the first intermediate **M** which dimerize to **D** once present in sufficient concentration. If free electron pair at amino nitrogen were engaged in a bond to Pd atom (present in **A**), one would expect blue shift instead of the red shift

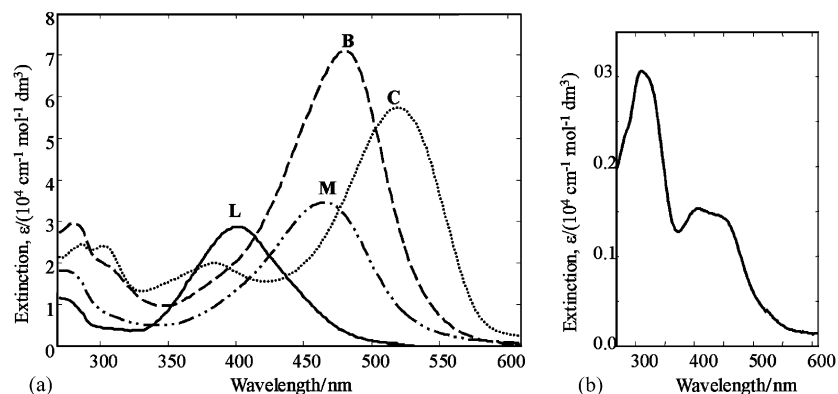


Fig. 2. Electronic absorption spectra of L, M, B, C in DMF (a) and A in CHCl_3 (b).

observed here. The intensity of this band at initial concentration of A $10^{-5} \text{ mol dm}^{-3}$ is decreasing monotonically during the reaction indicating the formation of only one species whose absorption occurs at 464 nm. Thus, the band at 464 nm corresponds to M. At initial concentration of A $10^{-4} \text{ mol dm}^{-3}$, the two-phase dynamics have been observed for this band during the whole course of reaction suggesting the formation of two species, most probably M and D, having strong absorption at very close positions.

The spectrum of B in DMF shows a very strong absorption band at 480 nm which probably includes contributions from metal to ligand charge transfer (MLCT) and two ligand transitions: spin-allowed $\pi-\pi^*$ and $n-\pi^*$. The second $\pi-\pi^*$ transition in the spectrum of B is located at the same position as in the free ligand (272 nm) suggesting that only the first $\pi-\pi^*$ transition of the ligand is affected by binding to palladium (Fig. 2a).

In the reaction of L and Na_2PdCl_4 isomers T_α and T_β were formed, where α and β denote which aza-nitrogen is bound to palladium. The presence of α and β species have been determined by $^1\text{H-NMR}$ spectra and this is described in the later sections 'reaction dynamics of ligand L with PdCl_2 ' and 'reaction dynamics of ligand L with Na_2PdCl_4 '. Since α isomer is four time more abundant than β isomer (Fig. 9), a prominent band observed at 451 nm in the spectrum of this reaction is assigned to $\pi-\pi^*$ and $n-\pi^*$ transitions of the bound ligand in T_α . A band corresponding to the second $\pi-\pi^*$ transition occurs in this spectrum at 279 nm.

The most intense band in the spectrum of C in DMF (520 nm) corresponds to the $\pi-\pi^*$ transition localized on the orthometallated ligand [3a,24]. Its intensity suggests that this transition is a charge-transfer in character. The band at 385 nm is interpreted as a ligand-field transition [3a]. The literature data on similar orthometallated Pd complexes [3a] suggest that one of the bands at 286 and 310 nm corresponds to the second $\pi-\pi^*$ transition localized on the orthometallated ligand (Fig. 2a).

3.1.3. Mass spectra

Positive and negative ion electrospray mass spectra were recorded by using DMF as a solvent in order to identify products and intermediates in the rearrangement reactions of A and B into C. Such analysis is possible since the ESMS technique enables transfer of preexisting ions from solution into the gas phase [25]. All electrospray mass spectra measurements were made with freshly prepared solutions as well as with the solutions that were left to stand for several hours having initial concentrations close to 10^{-4} and $10^{-5} \text{ mol dm}^{-3}$. In both cases (freshly prepared and old solutions) spectra were recorded continuously for 25 min. Peaks in the ES mass spectra were identified by the most intense m/z value within the isotopic mass distribution. There is a very good agreement between experimental and calculated m/z values.

The additional evidence for rearrangement of A into C is the presence of peaks due to ions of $[\text{C}+\text{H}]^+$ at m/z 1161 and $[\text{C}-\text{H}]^-$ at m/z 1159 in the positive and negative electrospray mass spectra of A, respectively (Fig. 3). At concentration close to $10^{-4} \text{ mol dm}^{-3}$ the spectra of A are characterized by the very fast changes in time and by the presence of peaks at higher m/z values (above 1000). In contrast, at concentrations close to $10^{-5} \text{ mol dm}^{-3}$ dominant peaks have m/z values under 1000 and spectral changes are much slower in time. The peak at m/z 1235 (1233) corresponds either to proto-

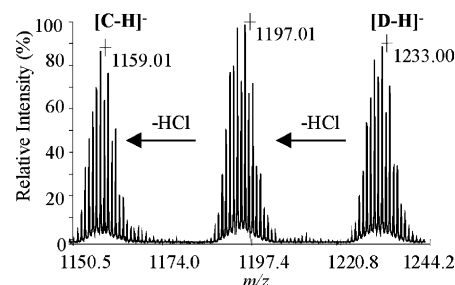


Fig. 3. Negative ion electrospray mass spectra of A recorded 10 min after dissolving in DMF.

nated (deprotonated) molecular ion of $[\text{PdCl}_2\text{L}]_2$ (**A**) or to intermediate complex $[\text{PdCl}(\mu\text{-Cl})\text{L}]_2$ (**D**).

The possibility that this peak is due to $[\text{A}\pm\text{H}]^\pm$ is excluded since in DMF solution the UV–vis and NMR results indicated immediate breaking of two Pd–N(amino) bonds and formation of intermediate **M** $[\text{PdCl}_2(\text{L})(\text{DMF})]$ which dimerize to **D** once present in sufficient concentration. So, the peak at m/z 1235 (1233) is due to protonated (deprotonated) molecular ion of **D** (Fig. 3). It should be pointed out that only this peak and peak at m/z 1199, formed by the loss of HCl from **D**, are present in the first spectrum of freshly prepared reaction solutions of **A** at concentration close to 10^{-4} mol dm $^{-3}$.

The formation of byproduct $[\text{PdCl}_3(\text{L})]^-$ (**T**) during the cyclopalladation reactions is also supported by the negative ion mass spectra of **A** which contain peak at 652 m/z corresponding to **T** (Fig. 4).

The spectra of freshly prepared solution of **B** change very slow in time if compared with the spectra of **A**. They contain only a weak peak at m/z 1057 corresponding to the protonated molecular ion of **B** and more intense peaks at m/z 1079 and 1095 due to $[\text{B}+\text{Na}]^+$ and $[\text{B}+\text{K}]^+$ ions, but not the peak at m/z 1161 corresponding to protonated molecular ion of **C** or peaks due to $[\text{C}+\text{Na}]^+$ or $[\text{C}+\text{K}]^+$ ions. The peak at m/z 1161 occurs in the spectra of several hours old solution of **B**. In the same spectra are also visible very weak peak at m/z 1235 corresponding to protonated molecular ion of **D**. The presence of the weak peak due to $[\text{C}+\text{H}]^+$ only in the spectra of several hours old solution of **B** is in accordance with results from UV–vis and NMR studies which indicate that the rearrangement of **B** into **C** proceeds at much slower rate than the rearrangement of **A**.

Complex **C** was identified by the presence of protonated molecular ion in the positive ion electrospray mass spectra at m/z 1061 and also by more intense peak at m/z 1183 assigned to ion $[\text{C}+\text{Na}]^+$.

Electrospray mass spectra gave reliable information on the species present in the solution. They support the proposed structures of complexes **B** and **C** as well as of the intermediates **M** and **D** and byproduct **T**.

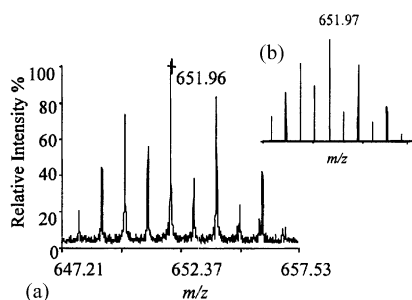


Fig. 4. Comparison experimental (a) and calculated (b) isotopic mass distribution for the $[\text{PdCl}_3\text{L}]^-$ (**T**) ion.

3.1.4. $^1\text{H-NMR}$ spectra

The $^1\text{H-NMR}$ spectra of **L**, **B**, **C**, intermediates **D** and **M*** and byproducts **T**, recorded in DMF, are given in Tables 2 and 3. The signal assignment was based on the chemical shifts and spin–spin couplings, two-dimensional experiments and on the comparison with the ^1H spectra of the related compounds [26]. $^1\text{H-NMR}$ spectra of **A** could not be obtained, not even at low temperature recording (-40°C) due to its fast rearrangement into **C**.

Coordination of the metal atom by α azo-nitrogen in **D $_\alpha$** and **B** and **T $_\alpha$** results in a large downfield shift of *ortho* protons H-9,11 and H-14,18. This shift is larger for protons H-9,11 although, in terms of bonds, protons H-14,18 are closer to the coordinating azo nitrogen (**N $_\alpha$**). This effect has been earlier observed and interpreted as paramagnetic anisotropy of the metal [21].

The reactions of **L** with Pd(II) compounds in DMF produce both α and β coordinated intermediates and byproducts. In both species H-9,11 were shifted stronger than H-14,18 and this shift was more pronounced in α -coordinated species (Tables 2 and 3). However, the spectrum of Pd(II) compounds with 4-methylazobenzene displays a reverse order of the two *ortho*-proton pairs [27]. Thus, it seems more plausible that the relative shifts of *ortho*-proton pairs are determined by the nature of *para*-substituent on the aromatic ring.

The positions of H-9,11 and H-14,18 signals of **D $_\alpha$** are very close to those of **T $_\alpha$** (Tables 2 and 3). The same was also observed for H-9,11 and H-14,18 signals of **D $_\beta$** and **T $_\beta$** . This suggests similar environment of H-9,11 and H-14,18 protons in **D $_\alpha$** and **T $_\alpha$** as well as in **D $_\beta$** and **T $_\beta$** (Scheme 1).

All protons in β -phenyl rings of the *ortho*-palladated complex **C** are non-equivalent due to the covalent bond of palladium with the *ortho*-carbon of β -phenyl ring. This bond causes a downfield shift of H-12 signal by 0.36 ppm and an upfield shift of H-8 and H-9 signals by 0.38 and 0.13 ppm, respectively, relative to the free ligand signals.

3.1.5. $^{13}\text{C-NMR}$ spectra in solution and in the solid state

$^{13}\text{C-NMR}$ data of **L**, **B**, **C** and byproducts **T** in DMF are summarized in Table 4. The signal assignment was ascertained by heteronuclear experiments. As complex **A** decomposes very fast in DMF solution, we have also recorded the solid-state ^{13}C cross-polarization-magic-angle spinning (CP-MAS) spectra of **A**, **L**, **B** and **C** (see Section 2).

The *ortho*-carbons C-9,11 and C-14,18 of all complexed species, except **C**, show the same shifts pattern as the analogous protons (Table 4). Signals of C-9,11 are always shifted downfield stronger than C-14,18 and this shift is also larger for α -coordinated species than for β -coordinated species. Except this, the most significant differences between α and β species were observed for

Table 2
¹H-NMR data in DMF (δ ppm, J Hz)

H	Compound			
	L	B	C $_{\alpha}$	D $_{\alpha}$ ^a
H-3	7.14 d $J(\text{HH}) = 8.0$	7.24 d $J(\text{HH}) = 8.1$	7.14 d $J(\text{HH}) = 8.0$	7.18 d $J(\text{HH}) = 7.7$
H-4	7.30 t $J(\text{HH}) = 7.6$	7.38 t ^b	7.31 t $J(\text{HH}) = 7.7$	7.35 t $J(\text{HH}) = 7.7$
H-5	6.98 t $J(\text{HH}) = 7.5$	7.06 t $J(\text{HH}) = 7.5$	7.00 t $J(\text{HH}) = 7.5$	7.04 t $J(\text{HH}) = 7.5$
H-6	7.74 d $J(\text{HH}) = 7.5$	^c	7.76 d $J(\text{HH}) = 7.5$	^c
H-8,12	7.20 d $J(\text{HH}) = 8.9$	7.40 d $J(\text{HH}) = 9.1$	6.88 d, br, 7.56 s ^d $J(\text{HH}) = 8.3$	7.49 d, br $J(\text{HH}) = 8.3$
H-9,11	7.91 d $J(\text{HH}) = 8.6$	9.52 d $J(\text{HH}) = 9.1$	7.78 d $J(\text{HH}) = 8.9$	9.98 ^e
H-14,18	7.96 d $J(\text{HH}) = 8.0$	8.47 br, d $J(\text{HH}) = 7.5$	8.2 d $J(\text{HH}) = 8.0$	8.88 d $J(\text{HH}) = 7.9$
H-15,17	7.70 t $J(\text{HH}) = 7.7$	^c	7.63 t $J(\text{HH}) = 7.6$	7.73 t $J(\text{HH}) = 8.0$
H-16	7.61 t $J(\text{HH}) = 7.2$	^c	7.58 d $J(\text{HH}) = 7.2$	^c
OH	10.46 s	10.56 s	10.47 s	10.61 s
NH	7.43 dd $J(\text{HH}) = 9.3$ ³ $J(\text{PH}) = 6.6$	8.61 dd $J(\text{HH}) = 8.9$ ³ $J(\text{PH}) = 6.6$	8.18 ^f	8.67 dd $J(\text{HH}) = 8.8$ ³ $J(\text{PH}) = 6.5$
PCH	5.70 dd $J(\text{HH}) = 9.3$ ² $J(\text{PH}) = 23.7$	5.89 dd $J(\text{HH}) = 8.9$ ² $J(\text{PH}) = 23.0$	5.81 dd, (5.73 dd) ^a $J(\text{HH}) = 9.3$, $J(\text{HH}) = 9.3$ ² $J(\text{PH}) = 22.8$, ² $J(\text{PH}) = 22.8$	5.87 dd $J(\text{HH}) = 9.0$ ² $J(\text{PH}) = 22.8$
OCH ₂ CH ₃	4.13 m ^g	4.22 m ^g	4.15 m ^g	4.16 m ^g
OCH ₂ CH ₃	1.25, 1.41 t $J(\text{HH}) = 7.0$	1.31, 1.45 t $J(\text{HH}) = 7.0$	1.28, 1.42 t $J(\text{HH}) = 7.0$	1.28, 1.44 t $J(\text{HH}) = 7.0$

^a The spectrum obtained by dissolving of **A** in DMF.

^b Partly overlapped with signal of H-8,12.

^c The signals of H-6, 15, 16, 17 are together overlapped in the range from 7.72 to 7.85 ppm.

^d H-8,12 are not equivalent in **C**.

^e Unresolved and broad doublet.

^f Overlapped with signal of DMF.

^g Centar of complex multiplet.

the carbons C-13 and C-10 which are the closest to the coordinating azo nitrogen atoms N $_{\alpha}$ or N $_{\beta}$ (Table 4).

The coordination of the metal atom by α azo-nitrogen atoms in **B** and **T $_{\alpha}$** causes downfield shift of C-13 (1.5 and 1.8 ppm, respectively) and upfield shift of C-10 (3.9 and 3.5 ppm, respectively) relative to the ligand. In the spectrum of byproduct **T $_{\beta}$** , upfield shift of C-13 carbon is 3 ppm while the signal of C-10 carbon shifts downfield for 1.6 ppm.

All carbons in β -phenyl rings of the *ortho*-palladated complex **C** show the similar shifts pattern as the analogous protons (Table 4). Only C-9 signal displays reverse shift (downfield by 8.3 ppm) in comparison with H-9. The largest downfield shift was observed for the

ortho-carbon C-11 (33.3 ppm) which is bound to palladium. This is in agreement with results reported for different cyclopalladated compounds [16c,16e].

It should be also pointed out that in all considered species the position of proton and carbon signals corresponding to the CH and (OCH₂CH₃)₂ groups are almost on the same place as in the free ligand. This excludes the possibility of coordination through the phosphoryl oxygen or amino nitrogen.

¹³C CP-MAS spectra confirmed solid-state structure of **A**. The significant shift of benzylic carbon signal (CH) was observed only in the spectrum of **A**. This signal, which is overlapped with two very close signals of CH₂ groups, moved downfield by ca. 16 ppm relative to the

Table 3
¹H-NMR data in DMF (δ ppm, J Hz)

H	Compound				
	D $_{\beta}$	T $_{\alpha}$	T $_{\beta}$	C $_{\beta}$ ^a	M $_{\alpha}^*$
H-9,11	9.07 d $J(\text{HH}) = 9.0$	10.08 d $J(\text{HH}) = 9.0$	9.16 d $J(\text{HH}) = 9.0$		9.42 d $J(\text{HH}) = 8.4$
H-14,18	8.88 dd $J(\text{HH}) = 7.9$	8.98 d $J(\text{HH}) = 7.8$	9.06 d $J(\text{HH}) = 7.8$		8.62 d $J(\text{HH}) = 7.8$
PCH	5.75 d $J(\text{HH}) = 9.3$ ² $J(\text{PH}) = 23.4$	5.83 dd $J(\text{HH}) = 9.2$ ² $J(\text{PH}) = 23.4$	5.73 dd $J(\text{HH}) = 9.4$ ² $J(\text{PH}) = 23.2$	5.66 dd $J(\text{HH}) = 9.2$ ² $J(\text{PH}) = 23.2$	5.86 dd $J(\text{HH}) = 9.0$ ² $J(\text{PH}) = 22.4$
OH	10.57 s	10.63 s	10.56 s		10.86 s
NH	^b	8.28 dd	^b		^b
CH ₃ SOCH ₃					3.59, 3.60 s

^a All signals of C $_{\beta}$ except of signal PCH proton overlapped with the signals of the other species present in solution.

^b Overlapped with aromatic protons.

Table 4
 ^{13}C -NMR data in DMF (δ ppm, J Hz)

C	Compound			
	L	B	C_α	T_α (T_β)
C-1	124.8	123.9	124.4	124.2 (124.5)
C-2	157.1 $^3J(\text{PC}) = 6.7$	157.0 $^3J(\text{PC}) = 6.4$	156.9 $^3J(\text{PC}) = 7.0$	157.5 (157.6) $^3J(\text{PC}) = 6.7$ (6.8)
C-3	116.8	116.7	116.8	116.8 (116.6)
C-4	130.6	130.7	130.5	130.7 ^a
C-5	121.0	121.0	120.8	120.9 (120.8)
C-6	130.7 $^3J(\text{PC}) = 5.2$	130.8 $^3J(\text{PC}) = 3.8$	130.8 $^3J(\text{PC}) = 3.4$	130.6 ^{a,b}
C-7	153.0 $^3J(\text{PC}) = 12.7$	156.1 $^3J(\text{PC}) = 12.4$	151.9 $^3J(\text{PC}) = 10.3$	155.5 (153.8) $^3J(\text{PC}) = 12.2$
C-8,12	114.6	114.9	114.3, 121.2 ^c	114.6 (113.5)
C-9,11	126.5	129.9	133.4, 159.8 ^c	129.8 (129.9)
C-10	145.8	141.9	156.2	142.3 (147.4)
C-13	154.7	156.2	152.9	156.5 (151.7)
C-14,18	123.5	125.7	125.8	126.5 (124.0)
C-15,17	130.9	130.4	129.8	130.0 ^a
C-16	131.4	131.5	130.0	131.3 (132.2)
PCH	48.8 $^1J(\text{PC}) = 156.7$	48.9 $^1J(\text{PC}) = 155.8$	48.7 $^1J(\text{PC}) = 155.2$	48.8 $^1J(\text{PC}) = 156.4$
CH_2CH_3	64.1, 64.3 $^2J(\text{PC}) = 6.9$	65.3, 64.5 $^2J(\text{PC}) = 7.0$	64.1, 64.2 $^2J(\text{PC}) = 7.0$	64.17, 64.4 $^2J(\text{PC}) = 7.0$
CH_2CH_3	17.3, 17.5 $J(\text{PC}) = 5.4$	17.4, 17.6 $J(\text{PC}) = 5.2$	17.3, 17.6 $J(\text{PC}) = 5.1$	17.3, 17.5 $J(\text{PC}) = 5.0$

^a The signals of T_β corresponding to C-4, 6, 15,17 are overlapped with the same signals of T_α and L in the range from 130.0 to 131.3 ppm.

^b Partly overlapped with the same signals of T_β and L and $^3J(\text{PC})$ could not be determined.

^c These carbons are not equivalent in C.

free ligand signal (48.6 ppm). Such a large shift can be only a consequence of the vicinity of metal ligation site and not the influence of surrounding molecules in the solid state. This is supported by the fact that the same signal in spectra of **B** and **C** moved upfield only for 1.5 and 2.6 ppm, respectively, relative to the free ligand signal. In **B** and **C** the metal ligation sites are not close to benzylic carbon and consequently changes in shift of benzylic carbon signal are much smaller than in **A**, in which each metal atom is coordinated by amino-nitrogen of one ligand and by azo-nitrogen (N_α) of another ligand (Scheme 1).

Solid-state ^{13}C spectra also supported the proposed structure of **B** and **C**. Although it is not possible to assign each signal in aromatic region the solid-state spectra of **L**, **B** and **C** are comparable with those recorded in DMF (see Section 2 and Table 4).

3.2. Mechanistic study

Upon dissolving in DMF, **A** and **B** rearrange into **C**, and the reactions reach equilibrium in 35 min or in a day, respectively. These reactions, and those between 1 mol equivalent of **L** and Pd(II) compounds, were studied by UV–vis spectroscopy monitoring the bands at 400, 464, 480 and 520 nm which correspond to the most intense transitions of **L**, **M**, **B** and **C** species, respectively. The same reactions were also followed by ^1H -NMR spectroscopy measuring intensities for several type of signals: (i) aromatic *ortho*-protons H-9,11 and H-14,18 (8.00–12.00 ppm); (ii) proton of CH group (5.60–5.80 ppm); and (iii) protons of CH_3 groups of free

and bound DMSO (3.20–3.70 ppm). All results support postulated solution dynamics presented in Scheme 1.

3.2.1. Reaction dynamics of complex A

UV–vis studies suggested that **A** is immediately solvolyzed in DMF producing two molecules of intermediate **M** [$\text{PdCl}_2(\text{L})(\text{DMF})$]. The monomer **M** is also susceptible to further solvolysis to **L** and at low concentration (ca. 10^{-5} mol dm^{-3}) this becomes a dominant process (Fig. 5). At higher concentration of **A** (ca. 10^{-4} mol dm^{-3}) monomer **M** either dimerizes to **D** or decomposes to **L**. Those two concurrent processes

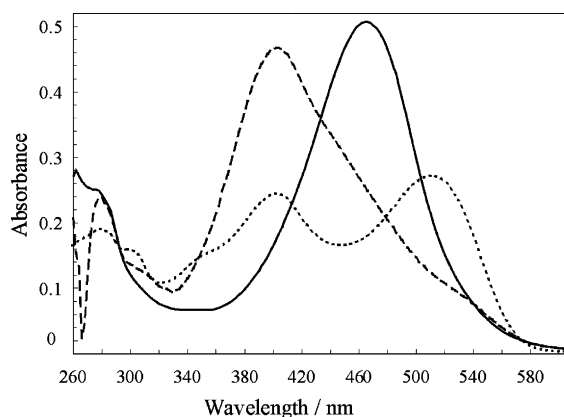


Fig. 5. Electronic spectra obtained by dissolving **A** in DMF with different starting concentrations: (—) freshly prepared solution of **A** (9.7×10^{-5} mol dm^{-3}); (···) the same solution 9.5 h later (in 0.1 cm cell); (---) the solution of **A** (9.7×10^{-6} mol dm^{-3}) 9.5 h after dissolution (in 1 cm cell).

occur at comparable rates (Fig. 5). Further increase in concentration promotes the formation of **C**.

Hence, the formation of **C** is (at least) a bimolecular process and most probably proceeds via: (i) immediate solvolysis of **A** producing the monomer **M**; (ii) subsequent dimerization of **M** into a chloro-bridged dimer **D**; which (iii) undergoes cyclopalladation and produces complex **C**. The presence of intermediate **D** is supported by the non-linear concentration dependence of the formation of **C** as well as by the electrospray mass spectrum obtained by dissolving **A** in DMF. The dimeric type intermediates have been already postulated in cyclopalladation reactions with *o*-tolylphosphane [28] and benzylamine [29] ligands.

The same reaction was studied by ¹H-NMR spectroscopy by recording spectra at regular intervals after dissolution of **A** in DMF. The most prominent features are presented in Fig. 6.

The two doublets (9.98 and 8.88 ppm) observed at the early stage of this reaction were attributed to H-9,11 and H-14,18 of dimer **D** since UV-vis and ESMS studies suggested that the equilibrium between intermediates **M** and **D** is shifted towards **D** if initial concentration of **A** was higher than 10⁻⁴ mol dm⁻³. Thus, it seems that the concentration of **M** is too low to be visible in NMR spectra. Such assignment is also supported by: (i) temporal profile of these signals (Fig. 6); (ii) their position in comparison with the position of analogous signals in **B**, **T** and **M*** species; and (iii) their presence in the reactions of PdCl₂ and PdCl₂(DMSO)₂ with **L** as well as in the reaction of **A** in DMF with addition a small amounts DMSO-*h*₆. At the early stage of the last

two reactions, we have also observed signals of monomer [PdCl₂(L)(DMSO)] (**M***) in addition to signals of **D** (see Section 3.2.4).

The intensity of signals of dimer **D** decreases very fast in time. This coincides with the dynamic of appearance of signal at 6.88 ppm corresponding to H-8 of **C** and signals at 10.08 and 8.98 ppm attributed to H-9,11 and H-14,18, respectively, of the monomer **T** [PdCl₃(L)]⁻.

Since signals of **T** are getting stronger as the signals of **D** got weaker, it was logical to conclude that byproduct was also formed from **D**. Our assumption is that chloride ions, released by cyclopalladation, react with **D** by splitting chloride-bridge and binding to palladium atoms to produce **T**. Thus, for each **C** molecule produced, two molecules of HCl are released and two molecules of **T** are formed. This is supported by the higher intensity of **T** signals if compared with the signals of **C**. The other possibility for the formation of **T** is replacement of DMF in **M** with the chloride ion. We have concluded that **T** is mainly produced by the reaction of **D** and chloride ions for two reasons: (i) **D** is present in much higher concentration and (ii) the rates of reactions of the bridged complexes are about two to three orders of magnitude faster than those for corresponding monomeric species [30]. The formation of monomeric species type [PdCl₃(L)]⁻ from dimeric complexes has been reported [30,31].

The presence of species **T** [PdCl₃(L)]⁻ in the reaction solution of **A** is confirmed by its negative ion electrospray mass spectra and occurrence in the other specific reactions (see below).

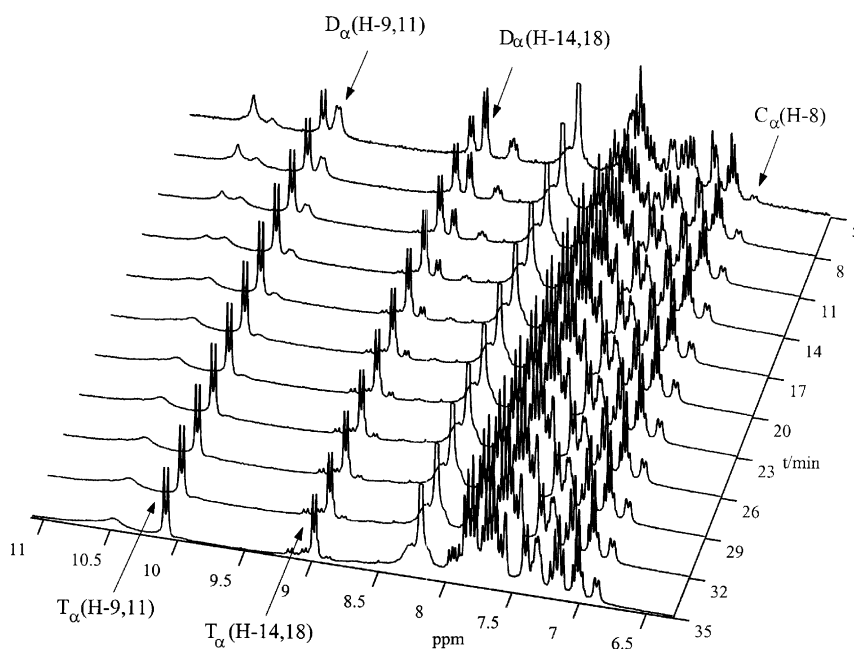


Fig. 6. ¹H-NMR spectra of **A** recorded immediately after dissolving in DMF.

3.2.2. Reaction dynamics of complex **B**

The formation rate of **C** from **B** is at least one order of magnitude slower than that from **A** because the coordinating bond between the metal and azo-nitrogen is more resistant to solvent attack than the coordinating bond with the amino-nitrogen.

The signals at 9.52 and 8.47 ppm correspond to the protons H-9,11 and H-14,18, respectively of **B** (Fig. 7). Their intensities slowly decrease in comparison to the analogue signals in the reaction of **A** (Fig. 6). The signals of **T** are visible and their temporal profile coincides with that of **C**, in accordance with the action of chloride ions released by cyclopalladation. Although signals of **D** are not observed, the presence of **T** signals suggests that **B** undergoes solvolytic reaction that produced **M** and **L** with further steps identical as in the solvolysis of **A** (Scheme 1). The proposed mechanism is additionally supported by: (i) the higher order concentration dependence of the solvolysis of **B**; and (ii) the electrospray mass spectrum of **B** which contains very weak peaks corresponding to protonated molecular ions of **M** and **D** intermediates.

3.2.3. Reaction dynamics of ligand **L** with PdCl₂

The higher order concentration dependence was also observed in the reaction of **L** with PdCl₂ in DMF. The formation of complex **C** was detected by UV–vis spectroscopy only at reactants concentrations higher than 10⁻⁵ mol dm⁻³.

At the early stage of this reaction (Fig. 8) the ¹H spectra contain two doublets (9.98 and 8.88 ppm) as the spectra of **A** and one additional doublet (9.07 ppm) with

the temporal profile corresponding to **D**. The doublet at 8.88 ppm corresponding to H-14,18 of **D** was two times greater than its analogous signal in **A**. These signals were explained as arising from two different dimeric species with Pd bound to N_α and N_β azo-nitrogens, respectively.

The formation of both species is a consequence of similar affinities of N_α and N_β azo-nitrogens towards palladium. This was additionally confirmed by the reactions of PdCl₂ with model azobenzene ligands. Only one isomer has been detected by ¹H-NMR spectroscopy for azobenzene and two for 4-aminoazobenzene and 4-methylazobenzene [27].

Thus, the signals at 9.07 and 8.88 ppm were assigned to H-9,11 and H-14,18, respectively, of the dimer with N_β coordination. Equal positions of the signals of H-14,18 in **D**_α and **D**_β explained the increase in intensity of one of the two **D**_α signals in comparison to those observed with **A** (Tables 2 and 3).

In the same reaction additional signals with the temporal profile of **T** were also observed, at 9.16 and 9.06 ppm. Logically, they were attributed to the **T**_β with N_β azo-nitrogen coordinating the metal atom, and specifically to the H-9,11 and H-14,18 protons, respectively. The signals of **T**_α and **T**_β were also observed in the reaction of **L** with Na₂PdCl₄ (see Fig. 9).

3.2.4. Reaction dynamics of ligand **L** with PdCl₂(DMSO)₂

In order to confirm the formation of monomeric and dimeric intermediates (**M** and **D**) on the path to **C** as well as the formation of byproduct type [PdCl₃L]⁻ we

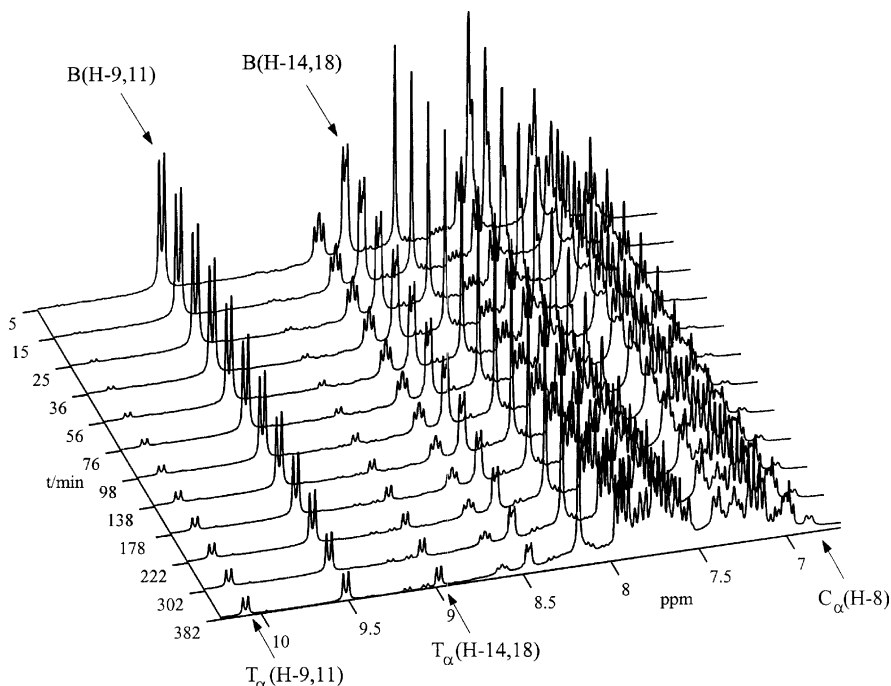


Fig. 7. ¹H-NMR spectra of **B** recorded immediately after dissolving in DMF.

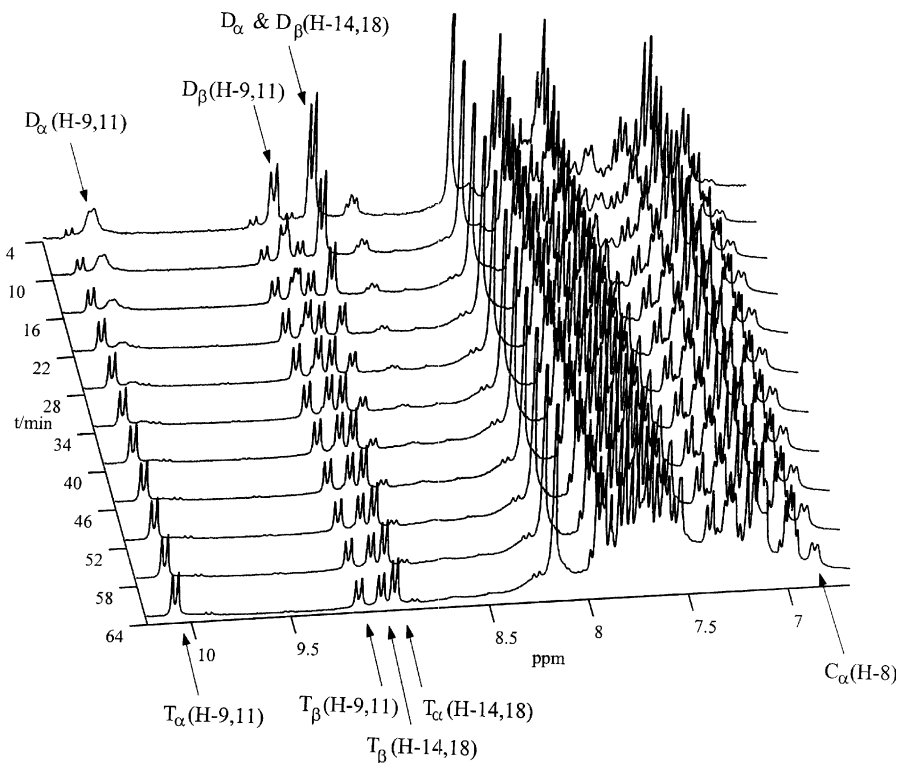


Fig. 8. $^1\text{H-NMR}$ spectra of the reaction of **L** with PdCl_2 recorded immediately after dissolving in DMF.

performed the reaction of **L** with $\text{PdCl}_2(\text{DMSO})_2$ complex in DMF.

The dissolution of $\text{PdCl}_2(\text{DMSO})_2$ in DMF produced a dimeric complex $[\text{PdCl}(\mu\text{-Cl})\text{DMSO}]_2$ which was

resolved and confirmed by its $^1\text{H-NMR}$ spectrum. The spectrum exhibits two separate peaks with equal intensities at 2.76 and 3.66 ppm, corresponding to free and bound DMSO molecules, respectively.

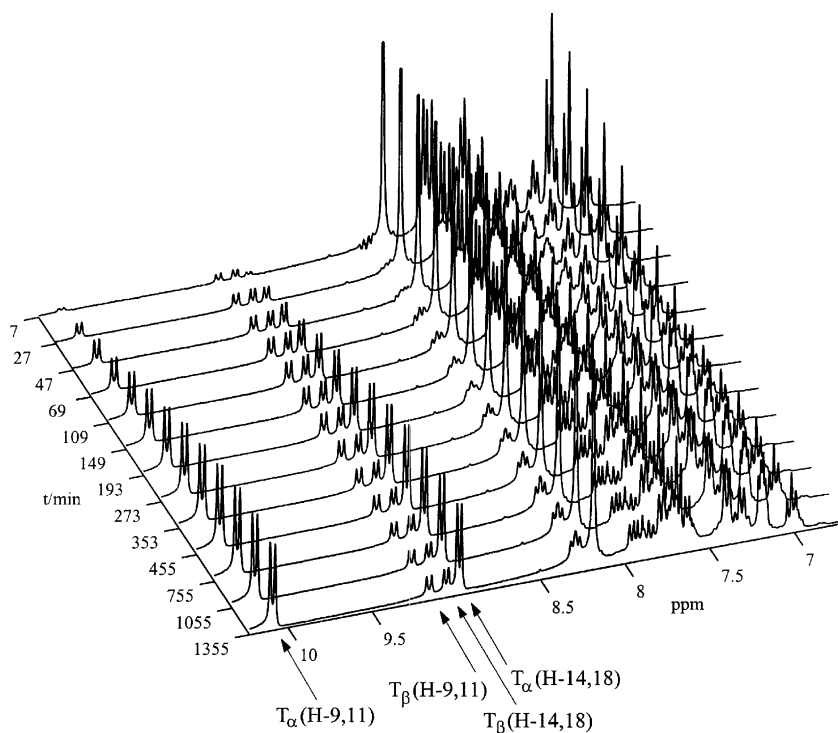
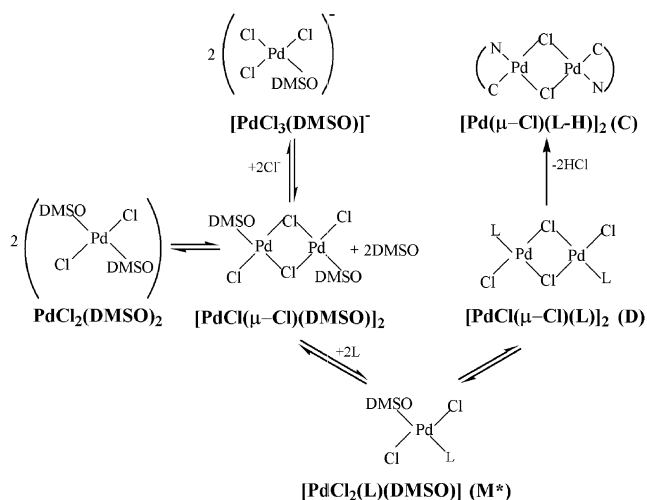


Fig. 9. $^1\text{H-NMR}$ spectra of the reaction of **L** with Na_2PdCl_4 recorded immediately after dissolving in DMF.



Scheme 2.

The formation of **C** in the reaction of **L** and $\text{PdCl}_2(\text{DMSO})_2$ proceeds *via* a similar mechanism as in reaction of **L** and PdCl_2 (Scheme 2). The initial dimer $[\text{PdCl}(\mu\text{-Cl})\text{DMSO}]_2$ was cleaved by **L** producing monomeric complex $[\text{PdCl}_2(\text{L})(\text{DMSO})]$ (**M***) that dimerizes into **D** if present in sufficient concentration. Complex **D** transforms rapidly into **C** releasing two HCl molecules.

The signals corresponding to monomeric species **T** are hardly visible in this reaction because the released chloride ions react with the initial dimer $[\text{PdCl}(\mu\text{-Cl})\text{DMSO}]_2$ producing new monomeric species $[\text{PdCl}_3(\text{DMSO})]^-$. The formation of this species is a result of the higher concentration of the initial complex than **D**, which transforms very fast into **C**. The signal of the bound DMSO in new species occur at 3.43 ppm and it was getting stronger as complex **C** is being formed. The formation of $[\text{PdCl}_3(\text{DMSO})]^-$ was checked by $^1\text{H-NMR}$ spectra of $\text{PdCl}_2(\text{DMSO})_2$ in DMF after addition of DCl. This produced the same signal at 3.43 ppm, while the signal at 3.66 ppm, corresponding to bound DMSO in the initial complex, has disappeared. The presence of signal at 3.43 ppm was also detected if DMSO- h_6 was added to DMF solution of Na_2PdCl_4 . In this case molecule of DMSO displaces chloride ion in Na_2PdCl_4 also producing $[\text{PdCl}_3(\text{DMSO})]^-$ species.

The presence of $\text{PdCl}_2(\text{L})(\text{DMSO})$ (**M***) as one of the intermediates on the path to **C** was indicated by occurrence of new signals at 9.42 and 8.62 ppm, attributed to H-9,11 and H-14,18, respectively with the same temporal profile as new signal of DMSO at 3.59 ppm.

The stronger coordinating affinity of DMSO in comparison with DMF was used to check the presence of cyclopalladated monomer $[\text{PdCl}(\text{L-H})(\text{DMF})]$ (**C/2**). DMSO- h_6 was added to a solution of **C** in DMF- d_7 prepared for recording $^1\text{H-NMR}$ spectra. During the next 15 days the signals of **C** and free DMSO- h_6 did not change at all.

3.2.5. Reaction dynamics of ligand **L** with Na_2PdCl_4

In this reaction molecule of **L** displaces chloride ion in Na_2PdCl_4 producing monomeric species **T**. T_α and T_β are formed at similar rates at the beginning of reaction, while at the later stage T_α becomes dominant (Fig. 9). This suggests that formation of T_α and T_β involves similar energy barriers and that T_α is thermodynamically more stable. The very weak signal corresponding to **C** was detected only after 2 days.

3.2.6. The formation of β -isomer of complex **C**

According to the proposed mechanism, whenever D_α and D_β were present, one would expect formation of C_α and C_β species, too. Indeed, this was confirmed in the reaction of **L** with PdCl_2 , by analyzing the PCH signals which occur isolated in the interval 5.60–5.90 ppm. At the end of the reaction there are five different PCH signals. They were interpreted by comparison with spectra of other studied solutions (obtained from **A**, **B** and from the reaction of **L** with Na_2PdCl_4). One of the signals was assigned to unreacted **L**, two corresponded to T_α and T_β , and another one was recognized as C_α , since it was present also in the reactions of **A** and **B** (where only α -species are present). The remaining signal was attributed to C_β since it has similar temporal dynamics as C_α . Significant overlap of signals corresponding to aromatic protons of both **C**-species (except H-8 of C_α) and all other species present in the solution prevented further assignment of signals in the range 7.00–8.00 ppm.

We believe that comparative study of the $^1\text{H-NMR}$ spectra recorded during the reactions of **A** and **B**, on one side, and during the reactions of **L** with PdCl_2 and Na_2PdCl_4 , on the other side, convincingly indicate formation of only α -species (D_α , T_α and C_α) in the first case, and formation of both α and β species ($\text{D}_{\alpha\beta}$, $\text{T}_{\alpha\beta}$ and $\text{C}_{\alpha\beta}$) in the second case.

3.2.7. The role of chlorides and protons in the reaction dynamics

As we mentioned earlier, two HCl molecules are released for each produced molecule of **C**. The released chlorides inhibit cyclopalladation reaction since they form stable monomer **T** by splitting the bridge in **D** or by replacing DMF in **M**. The monomer **T** undergoes the reactions of cyclopalladation and solvolysis but very slow. In the reaction of $\text{PdCl}_2(\text{DMSO})_2$ and **L** the released chloride ions and initial dimer form stable monomer $[\text{PdCl}_3(\text{DMSO})]^-$ which does not participate in the cyclopalladation reaction.

In all reactions where **C** was formed, the water signal is strongly shifted (Fig. 10) due to the interaction of water molecules with protons released during the cyclopalladation. In the reaction of **L** and Na_2PdCl_4 this signal remains almost at its initial position after 24

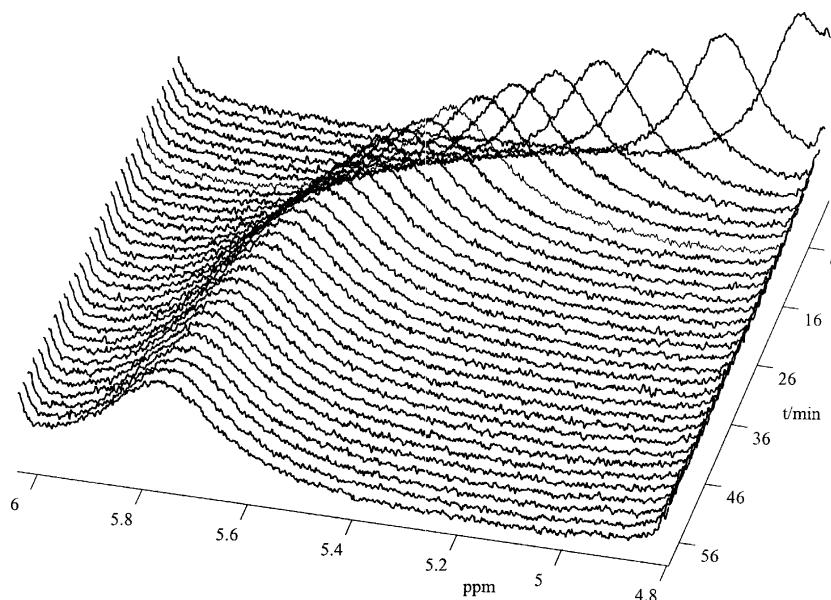


Fig. 10. $^1\text{H-NMR}$ spectra of the reaction of **L** with PdCl_2 showing the shift of the water signal due to the release of protons by cyclopalladation

h. Such a specific behavior of water signal was very helpful in the interpretation of reaction dynamics.

4. Conclusion

The dynamics presented in Scheme 1 should be considered as a complex equilibrium rather than as a set of individual reaction paths. Apart from two predominantly irreversible steps (solvolysis of **A** and cyclopalladation reaction) all other reactions are reversible. The cyclopalladated complexes **C** and **T** seem to be the most stable among all involved species. Complex **T** also enters the cyclopalladation reaction but very slowly, probably as a result of the electrostatic repulsion, which must be overcome in formation of **D** from two **T** ions. Although not directly confirmed yet, the dimer **D** seems to be the most unstable species. The formation of intermediate **D** on the way to **C** is clearly indicated by the non-linear concentration dependence of the cyclopalladation reaction.

Quantitative kinetic modeling, that we plan to perform, should provide additional arguments for the proposed mechanism. This is not possible with NMR signals alone since the relatively high measurement error of their intensities (approaching 10%) precludes accurate quantitative analysis. Besides, sufficiently intense NMR spectra can be obtained only at high concentrations, which cannot be varied much. UV–vis spectra provide more precise data for quantitative analysis but strong overlap of major bands makes deconvolution of individual spectra difficult.

Acknowledgements

The Ministry of Science and Technology of the Republic of Croatia (Grant no. 0098035) provided financial support for this research.

References

- [1] (a) A.D. Ryabov, *Synthesis* (1985) 233; (b) M. Pfeffer, *Recl. Trav. Chim. Pays-Bas* 109 (1990) 567.
- [2] (a) A. Bose, C.H. Saha, *J. Mol. Catal.* 49 (1989) 271; (b) R. Navarro, E.P. Urriolabeitia, C. Cativiela, M.D. Diaz-de-Villegas, M.P. Lopez, E. Alonso, *J. Mol. Catal.* 105 (1996) 111; (c) M. Camarago, P. Dani, J. Dupont, R.F. De-Souza, M. Pfeffer, I. Tkatchenko, *J. Mol. Catal.* 109 (1996) 127.
- [3] (a) Y. Wakatsuki, H. Yamazaki, P.A. Grutsch, M. Santhanam, C. Kutal, *J. Am. Chem. Soc.* 107 (1985) 8153; (b) R. Schwarz, G. Gliemann, P.H. Jolliet, A. von Zalevsky, *Inorg. Chem.* 28 (1989) 309.
- [4] (a) J. Albert, J. Granel, J. Sales, *Organometallics* 14 (1995) 1393; (b) G. Zhao, Q.G. Wang, T.C.W. Mak, *J. Chem. Soc. Dalton Trans.* (1998) 1241.
- [5] (a) M. Ghedini, D. Pucci, A. Crispini, G. Barberio, *Organometallics* 18 (1999) 2116; (b) M. Ghedini, D. Pucci, A. Crispini, G. Barberio, I. Aiello, F. Barigelletti, A. Gessi, O. Francescangeli, *Appl. Organomet. Chem.* 13 (1999) 565.
- [6] (a) C. Navarro-Ranniger, I. Lopez-Solera, J.M. Perez, J.R. Masaguer, C. Alonso, *Appl. Organomet. Chem.* 7 (1993) 57; (b) J.D. Higgins, *J. Inorg. Biochem.* 49 (1993) 149.
- [7] (a) J. Dehand, M. Pfeffer, *Coord. Chem. Rev.* 18 (1976) 327; (b) M.I. Bruce, *Angew. Chem. Int. Ed. Engl.* 16 (1977) 73; (c) I. Omae, *Chem. Rev.* 79 (1979) 287; *Coord. Chem. Rev.* 32 (1980) 235; 42 (1982) 245; 83 (1988) 137.; (d) G.R. Newkome, W.E. Puckett, V.K. Gupta, G.E. Kiefer, *Chem. Rev.* 86 (1986) 451; (e) J. Albert, M. Gomez, J. Granel, L. Sales, X. Solans, *Organometallics* 9 (1990) 1405; (f) P.L. Alsters, P.F. Engel, M.P. Hogerheide, M. Copijn, A.L.

- Spek, G. Van Koten, *Organometallics* 12 (1991) 1831;
- (g) J.M. Valk, F. Maassarani, P. Van der Sluis, A.L. Spek, J. Boersma, G. Van Koten, *Organometallics* 13 (1994) 2320;
- (h) J. Vicente, I. Saura-Llamas, M. Palin, P.G. Jones, C. Ramirez de Arellano, *Organometallics* 16 (1997) 826 (and references therein).
- [8] A.C. Cope, R.W. Siekman, *J. Am. Chem. Soc.* 87 (1965) 3272.
- [9] A.D. Ryabov, I.K. Sakodinskaya, A.K. Yatsimirski, *J. Chem. Soc. Dalton Trans.* (1985) 2629.
- [10] (a) T. Yagyu, S. Aizawa, S. Funahashi, *Bull. Chem. Soc. Jpn.* 71 (1998) 619;
- (b) T. Yagyu, S. Iwatsuki, S. Aizawa, S. Funahashi, *Bull. Chem. Soc. Jpn.* 71 (1998) 1857.
- [11] (a) M. Gomez, J. Granell, M. Martinez, *J. Chem. Soc. Dalton Trans.* (1998) 37;
- (b) M. Gomez, J. Granell, M. Martinez, *Organometallics* 16 (1997) 2539;
- (c) M. Gomez, J. Granell, M. Martinez, *Eur. J. Inorg. Chem.* (2000) 217.
- [12] R.P. Thummel, Y. Jahng, *J. Org. Chem.* 52 (1987) 73.
- [13] (a) G.W. Parshall, *Acc. Chem. Res.* 3 (1970) 139;
- (b) A.K. Yatsimirski, *Zh. Neorg. Khim.* 24 (1979) 2711.
- [14] M.I. Bruce, B.L. Goodall, G.A. Stone, *J. Chem. Soc. Dalton Trans.* (1978) 687.
- [15] (a) H. Takahashi, J. Tsuji, *J. Organomet. Chem.* 10 (1967) 511;
- (b) A.D. Ryabov, *Chem. Rev.* 90 (1990) 403.
- [16] (a) Lj. Tušek-Božić, I. Matijašić, G. Bocelli, G. Calestani, A. Furlani, V. Scarcia, A. Papaioannou, *J. Chem. Soc. Dalton Trans.* (1991) 195;
- (b) Lj. Tušek-Božić, M. Ćurić, J. Balzarini, E. De Clercq, *Nucleosides Nucleotides* 14 (1995) 777;
- (c) M. Ćurić, Lj. Tušek-Božić, D. Vikić-Topić, V. Scarcia, A. Furlani, J. Balzarini, E. De Clercq, *J. Inorg. Biochem.* 63 (1996) 125;
- (d) Lj. Tušek-Božić, A. Furlani, V. Scarcia, E. De Clercq, J. Balzarini, *J. Inorg. Biochem.* 723 (1998) 20;
- (e) Lj. Tušek-Božić, M. Komac, M. Ćurić, A. Lyčka, V. Scarcia, A. Furlani, *Polyhedron* 19 (2000) 937.
- [17] B.E. Winger, S.A. Hofstadler, J.E. Bruce, H.R. Udseth, R.D. Smith, *J. Am. Soc. Mass Spectrom.* 4 (1993) 566.
- [18] ICR-2LS software developed in Pacific Northwest National Laboratory, 902 Battelle Boulevard, Richland, WA 99352, USA.
- [19] Lj. Tušek, V. Jagodić, *Croat. Chem. Acta* 49 (1977) 829.
- [20] J.R. Doyle, P.E. Slade, H.B. Jonassen, *Inorg. Synth.* 6 (1960) 216.
- [21] R.J. Goodfellow, P.L. Goggin, *J. Chem. Soc. A* (1967) 1897.
- [22] (a) A.I. Balch, D. Petridis, *Inorg. Chem.* 8 (1969) 2247;
- (b) J.F. Van Baar, K. Vrieze, D.J. Stufkens, *J. Organomet. Chem.* 81 (1974) 247.
- [23] (a) H. Bisle, M. Romer, H. Rau, *Ber. Bunsen-Ges. Phys. Chem.* 80 (1976) 301;
- (b) H. Muströph, H. Epperlein, *J. Prakt. Chem.* 322 (1980) 305.
- [24] A.D. Ryabov, L.G. Kužmina, N.V. Dvortsova, D.J. Stufkens, R. Van Eldik, *Inorg. Chem.* 32 (1993) 3166.
- [25] R. Colton, B.D. James, I.D. Potter, J.C. Traeger, *Inorg. Chem.* 32 (1993) 2626.
- [26] Lj. Tušek-Božić, M. Ćurić, D. Vikić-Topić, A. Lyčka, *Collect. Czech. Chem. Commun.* 62 (1997) 1888.
- [27] D. Babić, M. Ćurić, Ž. Marinić, unpublished results.
- [28] M. Beller, T.H. Riermeier, S. Haber, H.J. Kleiner, W.A. Herrmann, *Chem. Ber.* 129 (1996) 1259.
- [29] J. Vicente, I. Saura-Llamas, M.G. Palin, *Organometallics* 16 (1997) 826.
- [30] F. Basolo, R.G. Pearson, *Mechanisms of Inorganic Reactions, A Study of Metal Complexes in Solution, II*, John Wiley and Sons, Inc, New York, 1967, p. 407.
- [31] M. Cusumano, A. Giannetto, P. Ficarra, R. Ficarra, S. Tommasini, *J. Chem. Soc. Dalton Trans.* (1991) 1581.